Water Quality Controllability Metrics, Limitations, and Hydraulic Dependencies

Salma M. Elsherif, S.M.ASCE[1]; Mohamad H. Kazma[2]; Ahmad F. Taha, Ph.D.[3]; and Ahmed A. Abokifa, Ph.D.[4]

[1]Dept. of Civil and Environmental Engineering, Vanderbilt Univ., Nashville, TN; Faculty of Engineering, Cairo Univ., Giza, Egypt; Email: salma.m.elsherif@vanderbilt.edu

[2]Dept. of Civil and Environmental Engineering, Vanderbilt Univ., Nashville, TN; E-mail: Mohamad.h.kazma@vanderbilt.edu

[3]Dept. of Civil and Environmental Engineering, Vanderbilt Univ., Nashville, TN; E-mail: ahmad.taha@vanderbilt.edu

[4]Dept. of Civil, Materials, and Environmental Engineering, Univ. of Illinois Chicago, Chicago, IL; Email: abokifa@uic.edu

ABSTRACT

Efficient water quality (WQ) control in distribution networks is pivotal for ensuring the delivery of safe and clean drinking water to consumers. Attaining this goal is complex due to the inherent intricacies of WQ systems, which often pose substantial challenges to achieving full controllability over their dynamics. Controllability, in this context, refers to the ability to effectively steer, regulate, and maintain disinfectant levels within the network to consistently meet the established water health standards. In addition, hydraulic conditions play a crucial role in influencing the level of WQ controllability. Hydraulic settings, including flow rates and directions, pressures, and network components, have a direct impact on how water quality dynamics propagate thereby influencing its controllability. In this study, we explore various metrics that provide both qualitative and quantitative assessments of water quality systems controllability. We examine the applicability of these metrics to the water quality systems taking into consideration network topology, booster stations' locations, and changes in hydraulic settings. By applying a comprehensive framework to various case studies, we assess the performance, practicality, and limitations of these metrics across different network configurations and scenarios. The outcomes of this assessment not only enable water system operators to evaluate the state of system controllability but also provide a pathway for leveraging these metrics to enhance the efficiency and effectiveness of control and regulation strategies.

INTRODUCTION

The control and regulation of water quality (WQ) in water distribution networks (WDNs) represent a critical and challenging process, relying on the unique nature of these systems and their intricate dynamics. The primary objective of WQ control problem is to maintain the standard disinfectant (i.e., chlorine) levels throughout the WDNs with minimal injections at treatment plants and booster stations (Fisher et al. 2018). An added challenge to this problem is the dependency of the WQ dynamics on the system's hydraulics, which influences the performance of the WQ controller. Several studies have covered the topic of controlling chlorine with various algorithms, objectives, and constraints (Ohar and Ostfeld 2014; Wang, Taha, and Abokifa 2021; Elsherif et al. 2024; Tryby et al. 2002). These studies have focused on obtaining the optimal chlorine injections to ensure meeting its standard residual levels with no further analysis on how to quantify the controller performance and coverage. In addition, these studies rely on the assumption that systems' hydraulics are pre-computed. Other studies acknowledge the interdependency between the system hydraulics and WQ dynamics and formulated a compact control problem (Abdallah and Kapelan 2019; Seyoum and Tanyimboh 2017; Drewa, Brdys, and Ciminski 2007; Ostfeld and Salomons 2006). In this compact problem, they solve for the optimal hydraulic operational settings while implicitly and/or explicitly incorporating one or more quality control aspects within the quantity control framework. This results in conflicting objectives and trade-offs between the quantity and quality aspects. Furthermore, incorporating a constraint on WQ, whether implicitly or explicitly, into the system's operational scheduling control problem does not necessarily guarantee the achievement of a certain level of controllability by booster stations or the reachability of the desired final states. That is, investigating the actual influence of the system hydraulics on the notion of WQ controllability has not been tackled in the literature and no quantitative measures have been defined nor employed, in this context, to judge the system behavior or to be utilized in improving it—a gap to be filled in this study.

To that end, the main objectives of this study are: *(i)* to introduce and explore the notion of WQ controllability from a system- and control-theoretic perspective—marking it as the first attempt, to the best of our knowledge; *(ii)* to introduce and validate the use of different quantitative controllability metrics on the WQ system, which allow us to judge the WQ system controllability from different energy-related perspectives; *(iii)* to examine the influence of system hydraulics on WQ controllability and understand how the controllability metrics reflect this impact; and *(iv)* to establish a pathway for utilizing these metrics to enhance WQ controller performance, address the operational hydraulic problem with a preview of how the outcomes can enhance the WQ controllability status, and perform booster station placement. This final objective contributes valuable insights during the planning phase of the WDNs, i.e., the booster stations placement procedures and for enabling WDN operators to efficiently manage systems that meet required quantity and quality standards. This is grounded in the comprehensive understanding of underlying interactions and potential improvements from a control standpoint.

METHODS

Herein, a model is introduced that tracks chlorine concentrations in the different WDNs components: reservoirs, junctions, tanks, pumps, valves, and pipes, along with the dynamics associated with injecting chlorine into the system by means of the booster stations distributed across the network. Next, we explain the construction of the controllability Gramian, a pivotal tool for evaluating the WQ controllability. Then, we explore the different controllability metrics. We note that, as we explore the impact of the hydraulics states on WQ controllability, we conduct multiple case studies for the test networks under diverse hydraulic scenarios. The hydraulic states, involving flow rates, heads, and velocities, are determined using the EPANET toolkit in MATLAB (Rossman et al. 2020). Note that, the simulation time scale for the hydraulics is different than the WQ one. The hydraulic time-step Δt_{H} is taken within an hourly scale, aligning with consumer demand updates, while the WQ time-step Δt_{WQ} is chosen between minutes and seconds to allow stable accurate numerical simulations (Seyoum and Tanyimboh 2017). That is, for a simulation window of $[0, T_{\mathrm{s}}]$, variable t presents a specific time and is updated incrementally by Δt_{WQ} within each Δt_{H} reaching the end of the simulation period at $t = T_{\mathrm{s}}$.

Water Quality Single-species Model

This model tracks chlorine concentrations across the network's components, governed by the principles of mass conservation, transport, and single-species reaction and decay models. The single-species decay model is a first-order model where chlorine decays linearly due to wall and bulk reaction dynamics. Transport and reaction in pipes are modeled using the advection-reaction partial differential equations (AR-PDEs) and solved using numerical discretization schemes that segment each pipe into a fixed spatiotemporal grid. The mass balance principle is applied to other network components. For brevity, we do not list the detailed equations for each component. The reader is referred to the study (Wang, Taha, and Abokifa 2021) for the governing equations of the WQ single-species model and how to concatenate them into a state-space representation. Notably, the one difference between that study's model and our model in this paper is the numerical method used to discretize the AR-PDEs. In this paper, we employ the explicit upwind Eulerian scheme (Elsherif et al. 2024), chosen for its accuracy in representing the physical aspects of the AR process when meeting the necessary stability conditions (Elsherif et al. 2023). To that end, the state-space representation capturing the chlorine evolution and booster stations is formulated in Eq. (1) as follows

$\mathbf{x}(t + \Delta t$ [redacted] $= \mathbf{A}(t)\mathbf{x}(t) + \mathbf{B}(t)\mathbf{u}(t),$ [redacted]

where $\boldsymbol{x}(t)$ is the vector depicting the chlorine concentrations in the entire network: reservoirs, junctions, tanks, pumps, valves, and each segment of each pipe; vector $\boldsymbol{u}(t)$ is the control inputs into the system (i.e., chlorine dosages by booster stations); and $\boldsymbol{A}(t)$ and $\boldsymbol{B}(t)$ are time-varying matrices. These matrices depend on the network topology and components characteristics, interdependency between the dynamics at the different components and booster stations, chlorine decay coefficient rate, and hydraulic states and parameters.

Water Quality Controllability Gramian and Metrics

In this section, we introduce the notions of controllability of linear water quality dynamics (Eq. (1)). Controllability is generally defined as the ability to steer or direct a system from an initial state x_0 to a final state x_f under the action of a control input u (Kalman 1963). In the context of water quality control, we want to be able to steer the chlorine concentrations to maintain residual levels that comply with EPA regulations (Acrylamide 2009). From a control-theoretic perspective, the dynamic linear system is said to be controllable if only if the controllability matrix $\boldsymbol{\mathcal{C}}_{\boldsymbol{N_s}}$ for N_s time-steps is full rank, i.e., $\mathrm{rank}\left(\boldsymbol{\mathcal{C}}_{\boldsymbol{N_s}}\right)$ equals the total number of system states (Hespanha 2018). This condition is known as Kalman's rank condition where the controllability matrix can be written as follows

$$\boldsymbol{\mathcal{C}}_{\boldsymbol{N_s}} \coloneqq \{\mathbf{B}, \mathbf{AB},\ \mathbf{A}^2\mathbf{B}, \dots, \mathbf{A}^{N_s-1}\mathbf{B}\}. \qquad \text{[redacted])}$$

This controllability measure is informative from a qualitative sense, however, it fails to provide a quantitative measure regarding the degree of controllability. Quantifying the level of controllability helps understand the change in the level and direction of controllability of a system under different operating conditions. To provide more practical measures, we refer to the use of the controllability Gramian $\boldsymbol{W}_c$. The Gramian, in the context of water quality control, provides information regarding the coverage of the chlorine injections across the network states and the control energy available to reach a desired level of chlorine residuals. The water quality controllability Gramian (WQ-CG) is calculated depending on the controllability matrix (Eq. [redacted])) and expressed as

$$\boldsymbol{W}_c = \sum_{\tau=0}^{N_s-1} \boldsymbol{A}^{\boldsymbol{\tau}}\boldsymbol{B}\boldsymbol{B}^{\top}(\boldsymbol{A}^{\boldsymbol{\tau}})^{\top} = \boldsymbol{\mathcal{C}}_{\boldsymbol{N_s}}\boldsymbol{\mathcal{C}}_{\boldsymbol{N_s}}^{\top}. \qquad \text{([redacted]}$$

To extract the aforementioned information from the controllability Gramian, a myriad of measures and metrics can be used (Pasqualetti, Zampieri, and Bullo 2014; Summers, Cortesi, and Lygeros 2016). These metrics provide a scalar energy-related quantification of the controllability Gramian. In our study, we cover the following quantitative metrics: $\log\det(\boldsymbol{W}_c)$, $\mathrm{trace}(\mathbf{W}_c^{-1})$, $\mathrm{trace}(\boldsymbol{W}_c)$, $\mathrm{rank}(\boldsymbol{W}_c)$, and minimum eigenvalue $\lambda_{\min}(\boldsymbol{W}_c)$. The $\log\det(\boldsymbol{W}_c)$ measure the volume of the ellipsoid enclosing the set of states that can be reached with at most a unit control energy input. This means that by increasing this value, the system is more controllable. The $\mathrm{trace}(\mathbf{W}_c^{-1})$ is proportional to the average energy required to drive the system from initial state x_0 to a final state x_f; it is infinite when one of the directions is not controllable. The $\mathrm{trace}(\mathbf{W}_c)$ is inversely related to the energy required to steer the system; it provides an overall measure of the controllability energy. The $\mathrm{rank}(\boldsymbol{W}_c)$ provides a qualitative measure of controllability by providing the size of the controllable subspace, in other words, how many states of the system is controllable. We note here that $\boldsymbol{W}_c$ is non-singular if the system is controllable for N_s time-steps, otherwise, it is uncontrollable. The minimum eigenvalue $\lambda_{\min}$ $(\boldsymbol{W}_c)$ is inversely proportional to the system's control energy; it quantifies the direction that requires the largest amount of energy. A more thorough discussion on the aforementioned metrics is presented in (Summers, Cortesi, and Lygeros 2016). We note that, for an uncontrollable system, we can employ the energy-oriented metrics on the controllable *subspace* of the system by applying decomposition approach, readers are referred to (Datta 2004) for the decoposition theorem.

CASE STUDIES

In our study, we test the controllability metrics performance and their dependency on the system's hydraulics and other unique factors on three test networks (Figure 1). The simplest of the three networks is the Three-node network, which consists of a reservoir, a pump, a junction, a pipe, and a tank. The 8-node and FFCL-1 networks are from the EPANET Users Manual (Rossman et al. 2020). The 8-node network has a reservoir, a pump, 6 junctions, 8 pipes, and a tank. Lastly, The FFCL-1 network is based on the Fairfield, California, water distribution system. FFCL-1 network includes a tank, 108 junctions, and 121 pipes. In addition, booster stations are distributed on nodes for each network as shown in Figure 1. Some booster stations have fixed locations for all simulation scenarios (colored in blue), while others are placed at specific locations for particular case study scenarios (colored in maroon and labeled with the corresponding case study number).

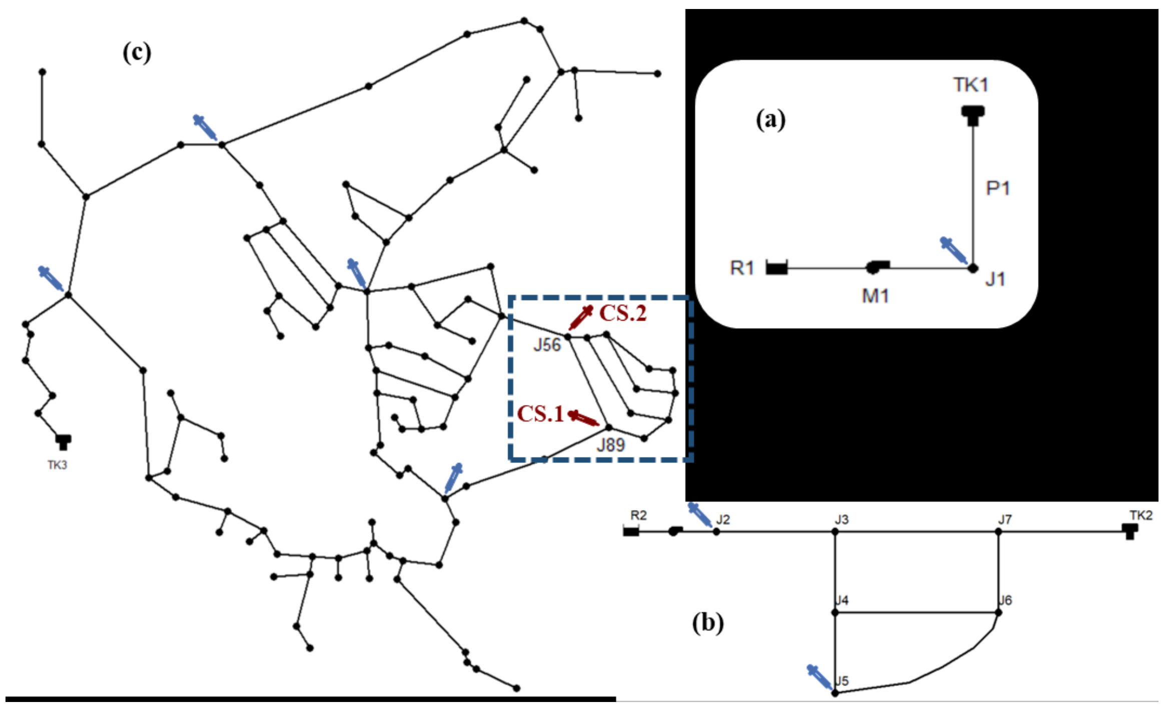

Figure 1. (a) Three-node, (b) 8-node, and (c) FFCL-1 (with a focused-on zone) networks. Booster stations are distributed across these networks, stations colored in blue are considered in all scenarios, whereas those in maroon are considered for specific case studies numbered and marked next to them.

Assessing Water Quality Controllability: Metrics Implementation

First, we assess the applicability and validity of the proposed metrics in reflecting the system's WQ controllability. Considering the Three-node network as a test case, there is one booster station located at J1. Pipe P1 is divided into 100 segments resulting in a total of 104 states. The WQ-CG is calculated within every hydraulic time-step of one hour. To facilitate the judgment of the Gramian rank, we calculate the percentage of the WQ-CG rank in relation to the total number of network states, providing representative insights into the controllability coverage. It is important to note that our analysis excludes Reservoir R1 and Pump M1 from the assessment as they are upstream of the booster station located at J1. This exclusion allows us to focus on evaluating the metric results specifically within the subspace of interest (J1-P1-TK1). For a total simulation period of 24 hours, Figure 2a illustrates the percentage (%) of the system's WQ-CG rank out of the number of states and the corresponding velocities at Pipe P1. In this scenario, positive velocities indicate the flow direction from J1 to TK1, while negative velocities reflect water flowing in the opposite direction. The flow direction in P1 is dependent on the demand pattern at J1 for this hydraulic setting and the head at TK1 which results in TK1 alternating between filling and emptying states. Results show that with higher velocities, chlorine injections from the booster station manage to reach a higher number of states and accordingly the WQ-CG rank increases reaching full controllability for some of the time steps. Conversely, at time-steps with negative velocities, the only covered state is J1 and the corresponding WQ-CG rank is less than 1%. That is, during these time-steps, the booster station does not contribute in achieving the desired chlorine residual levels.

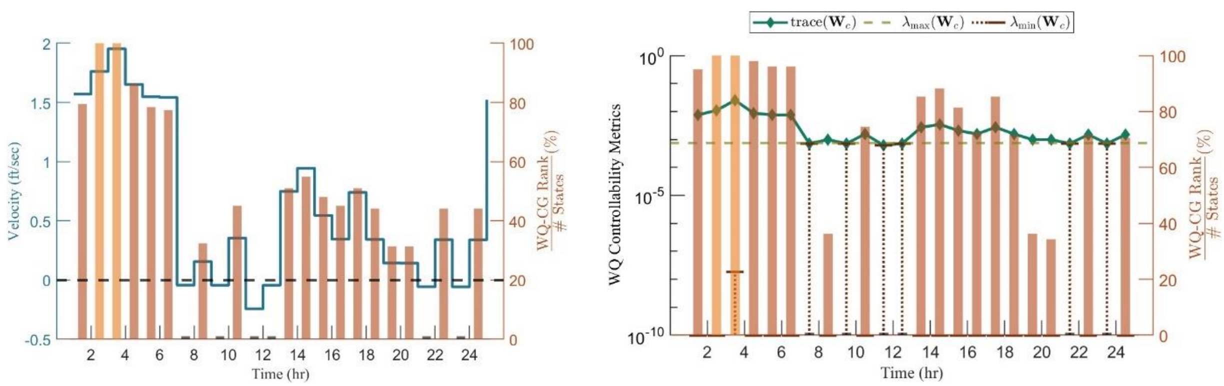

(a) **(b)**

Figure 2. [redacted]ater velocity in Pipe P1 of the Three-node network and the corresponding WQ-CG [redacted]n ratio to the total number of states in the system (%). Positive velocities represent[redacted]low direction from Junction J1 to Tank TK1, while the negative velocities reflect water flowing in the opposite direction. (b) The correspondent metrics: trace, $\lambda_{\min}$, and $\lambda_{\max}$ of the WQ-CG for this hydraulic scenario.

For the same hydraulic simulation, Figure 2b demonstrates the WQ-CG [redacted] and minimum eigenvalue $\lambda_{\min}$ for each hydraulic time-step. Additionally, the maximum eigenvalue $\lambda_{\max}$ of the Gramian is depicted as a horizontal line, remaining constant throughout the entire simulation. The reason $\lambda_{\max}$ does not change is that we only have one booster station at J2, with a single energy direction through P1 defining the direction with [redacted]ighest stored energy. It is noticeable that the higher the rank of the WQ-CG, the greater the [redacted]as well. However, the trace only reflects the *average* controllability of the subspace without providing information on how this energy is distributed along the control directions. To that end, the minimum eigenvalue $\lambda_{\min}$

is the metric used to measure this information. As illustrated in Figure 2b, there exists a control direction with low controllability energy required to reach specific states' values for the whole simulation window except for the third hour. Nevertheless, for time steps with negative velocities, all the energy is stored in J2, resulting in the minimum e[redacted]alue λ_{min} being equal to the maximum eigenvalue λ_{max}, which, in turn is equivalent to the [redacted]of the WQ-CG.

It [redacted]rth [redacted]ing that for all simulations presented in the case studies section, the WQ-CG [redacted]and [redacted]metrics give the same values. This observation implies that either of these metrics can be effectively employed to judge the controllability energy stored in the WQ [redacted]y the distributed bo[redacted]onetheless, it is recommended to utilize the [redacted]etric rather than the [redacted]ssessing the WQ controllability. The rationale behind this suggestion is that the WQ dynamics have a large number of states, a consequence of discretizing the pipes for a stable and accurate representation—the simple Three-node network has 104 states. Accordingly, the dimension of the WQ-CG is also high, which adds to the computational burden, as calculating the inverse of such a high-dimensional Gramian poses a significant computational challenge.

Hydraulics Influence on Water Quality Controllability

In this section, we explore the influence of variations in hydraulic settings on WQ controllability. This is achieved by comparing metrics values across different scenarios. Specifically, alterations in consumers' demand values and patterns at the junctions of the 8-node network are examined, resulting in three distinct hydraulic scenarios. The simulation duration spans 24 hours, with a one-hour hydraulic time-step and a 10-second WQ time-step applied across all scenarios. The 8-node network has two booster stations located at J2 and J5 as shown in Figure 1.

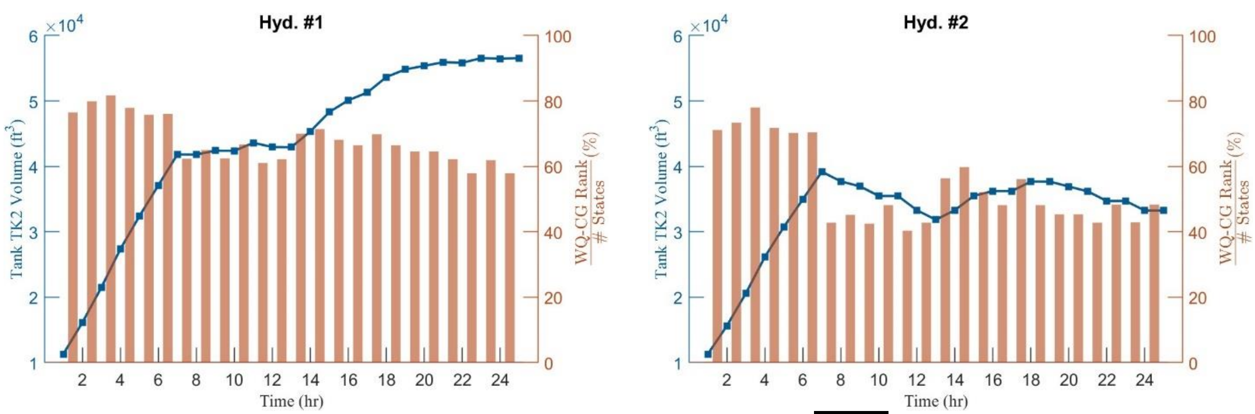

Figure 3. Tank TK2 volume vs. the corresponding WQ-CG [redacted]n ratio to the total number of states in the system (%) of the 8-node network for two different hydraulic scenarios.

Figure 3 demonstrates the T[redacted]olume for the first two hydraulic scenarios (Hyd. #1 & #2) and the corresponding WQ-CG [redacted]n ratio to the total number of states. For both scenarios, TK2 undergoes filling during the initial 7 hours of the simulation, with an approximate equivalent controllability coverage. Under such scenarios, water is flowing from J6 to J5, accordingly, it is unaffected by the chlorine injections at J5. Additionally, under the flow velocities of the these scenarios, the results show that this part of the network is not reachable by the injections at J2 within the 1-hr hydraulic time-step. That is, the system is not fully controllable for both scenarios up till the 7th hour of simulation. For the remainder of the 24-hour simulation window, the majority of the time steps involve w[redacted]being withdrawn from TK2 in Hyd. #2, in contrast to Hyd. #1. Consequently, the WQ-CG [redacted]s lower for Hyd. #2 scenario between the 7th and 24th hours as flow directions in pipes [redacted] unreachable zones by the booster stations injections. However, the average controllability energy distributed between the controllable states for Hyd. #2 is higher as depicted in Figure 4b. This energy is influenced by the actual water velocities in pipes for each scenario not only the direction. Furthermore, Figure 4a shows the change in TK2 volume [redacted] third hydraulic scenarios in comparison to the first two scenarios, along with the WQ-CG [redacted] Figure 4b. In Hyd. #3 scenario, the head at TK2 reaches equilibrium with the head at J7 after the 9th hour of simulation. This results in no flow in the connecting pipe and no change in TK2 volume for the rest of the simulation window. After the 9th hour, [redacted] controllability coverage is the same for Hyd. #2 and #3 scenarios. Nonetheless, the WQ-CG [redacted] values are higher for the Hyd. #3 scenario since the actual hydraulics (i.e., flow rates and [redacted]) in the system result in a higher stored energy that is used to steer the chlorine concentrations to a desirable value.

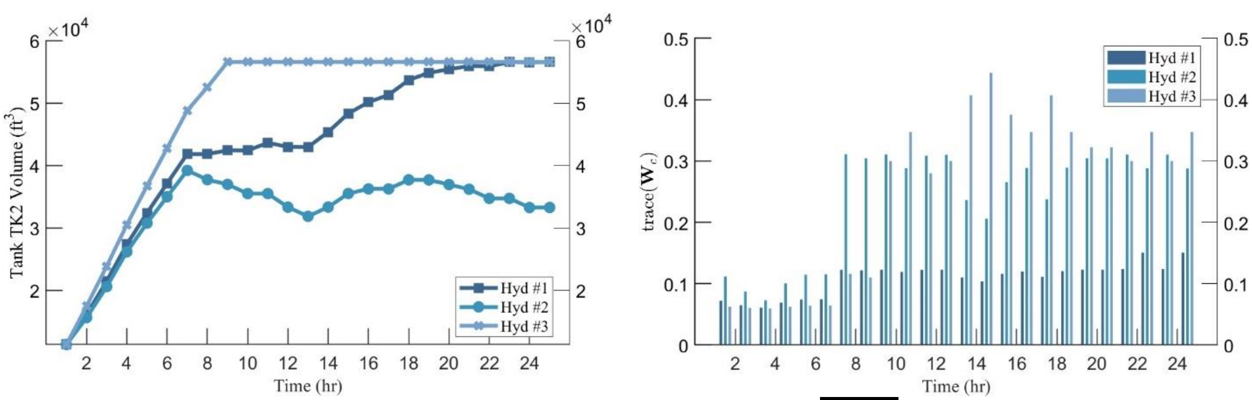

(a) **(b)**

Figure 4. Tank TK2 volume vs. the corresponding WQ-CG [redacted] of the 8-node network for three [redacted] scenarios.

In conclusion, each of the [redacted] and λ_{min} metrics reflects an important behavior of the WQ dynamics [redacted] consideration when investigating the reachability of desired controllability levels across the system. Furthermore, these metrics are significantly impacted by the system hydraulics, showcasing a significant potential for enhancing WQ controllability by aligning it with the specific hydraulics of the system resulting in a more efficient WQ regulation.

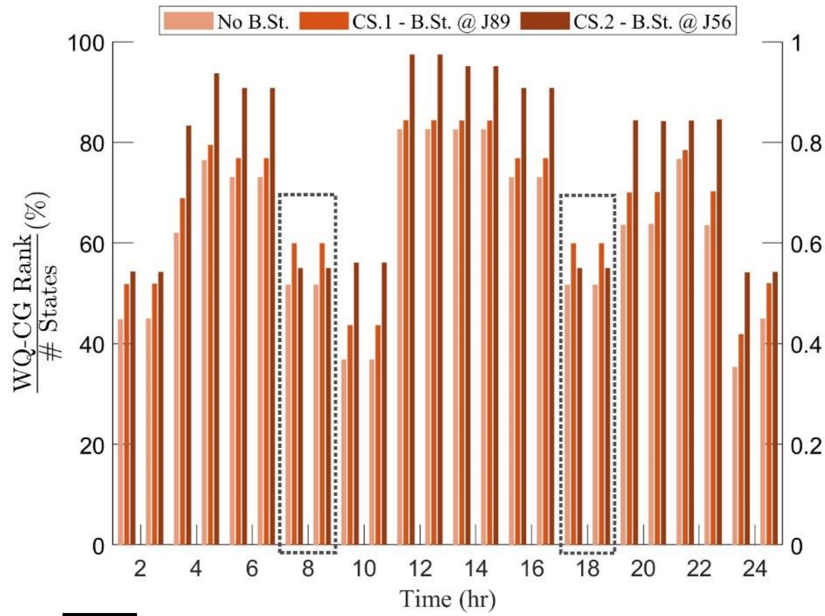

Figure 5. WQ-CG [redacted]n ratio to the total number of states of the FFCL-1 network (%) for three different [redacted] studies. The first case study has no booster station (B.St.) in the focused-on zone, the second case study has a booster station at J89, and the last one has a booster station at J56.

Analyzing Water Quality Controllability through Variable Booster Station Placement

Lastly, we evaluate utilizing WQ controllability metrics on the FFCL-1 network and investigate the impact of changing the booster station placements across the network. FFCL-1 has a unique topology with several dead-ends and water flowing under pressure driven by gravity energy sourced from Tank TK3. FFCL-1 network has four fixed booster stations and two additional stations considered for specific case studies, referred to as CS.1 and CS.2, as illustrated in the focused-on zone of the network in Figure 1. We examine the scenario where there is no booster station in this zone as the base configuration, which is subsequently u[redacted] by the addition of a booster station at either J89 or J56. We simulate over a 24-hour period [redacted]1-hr hydraulics time-step and a 1-min WQ time-step. Results exhibit an increase in both the [redacted]and trace of the WQ-CG upon the addition of a booster station at either J89 or J56, which ref[redacted]e low controllability coverage over that zone when only the four fixed booster stations are utilized—refer to Figure 5. On the other [redacted] for the majority of the simulation period, placing the booster station at J56 yields higher [redacted]and $trace$ values than at J89, except for the two specific time windows framed in**Figure 5**. T[redacted]esults stem from the change in flow directions in this looped zone during those time windows so that the booster station at J89 injections has more domination, thereby emphasizing the impact of booster station placement on controllability dynamics. Hence, our investigation can be facilitated to adopt a reverse approach, where these metrics are utilized under various possible hydraulic scenarios for each network to allow for the efficient selection of booster station locations that not only maximize WQ controllability coverage over system states but also enable effective steering of chlorine residuals to sufficient levels.

CONCLUSIONS

This study conducts a comprehensive analysis of implementing controllability metrics for WQ dynamics. This analysis is performed on three test networks with different topologies and scales, under various hydraulic scenarios. The results o[redacted] analysis highlight the distinctions between metrics in terms of their quantified aspects. The [redacted] metric provides informati[redacted] the controllability coverage by the booster stations distributed across the network, whereas [redacted] and logdet metrics assess the energy associated with steering the chlorine concentrations to a desirable state by these s[redacted]s injections with a least energy control direction defined by the λ_{min} metric. Note that, the [redacted] and logdet metrics provide same insights for the WQ linear dynamics and accordingly either of them can be utilized depending on the comput[redacted]l methods used or the problem to be solved. Lastly, the study recommends employing the [redacted] metric on the Gramian rather than its inverse for WQ controllability assessment due to computational complexities associated with the high dimensionality of discretized WQ dynamics, making the inverse calculation impractical for large networks.

That is, the [redacted] [redacted] logdet and λ_{min} metrics offer valuable insights for assessing WQ controller performance according to their measures and allow us to plan accordingly. The study reveals the direct influence of system hydraulics on these metrics and WQ controllability. This conclusion paves the way for future work to integrate these metrics while solving the hydraulic operational problem in order to obtain settings that satisfy consumers' needs and also attain sufficient/desirable levels of WQ controllability. Furthermore, future work could extend the investigation and implementation of those metrics to tackle the booster station placement problem which directly defines the WQ system control performance and limitations.

ACKNOWLEDGMENT

This work is supported by the National Science Foundation under Grant 2151392.

REFERENCES

Acrylamide, O. C. 2009. “National Primary Drinking Water Regulations.” *Kidney* 2 (4-D): 0.07.

Datta, Biswa. 2004. *Numerical Methods for Linear Control Systems*. Academic Press.

Elsherif, Salma M., Ahmad F. Taha, Ahmed A. Abokifa, and Lina Sela. 2024. “Comprehensive Framework for Controlling Nonlinear Multispecies Water Quality Dynamics.” *Journal of Water Resources Planning and Management* 150 (2): 04023077. https://doi.org/10.1061/JWRMD5.WRENG-6179.

Elsherif, Salma M., Shen Wang, Ahmad F. Taha, Lina Sela, Marcio H. Giacomoni, and Ahmed A. Abokifa. 2023. “Control-Theoretic Modeling of Multi-Species Water Quality Dynamics in Drinking Water Networks: Survey, Methods, and Test Cases." *Annual Reviews in Control* 55: 466–85.

Fisher, Ian, George Kastl, Feng Shang, and Arumugam Sathasivan. 2018. "Framework for Optimizing Chlorine and Byproduct Concentrations in Drinking Water Distribution Systems." *Journal: American Water Works Association* 110 (11).

Hespanha, João P. 2018. *Linear Systems Theory*. 2nd edition. Princeton: Princeton University Press.

Kalman, Rudolf Emil. 1963. "Mathematical Description of Linear Dynamical Systems." *Journal of the Society for Industrial and Applied Mathematics, Series A: Control* 1 (2): 152–92.

Ohar, Ziv, and Avi Ostfeld. 2014. "Optimal Design and Operation of Booster Chlorination Stations Layout in Water Distribution Systems." *Water Research* 58: 209–20.

Pasqualetti, Fabio, Sandro Zampieri, and Francesco Bullo. 2014. "Controllability Metrics, Limitations and Algorithms for Complex Networks." *IEEE Transactions on Control of Network Systems* 1 (1): 40–52. https://doi.org/10.1109/TCNS.2014.2310254.

Rossman, L. A., H. Woo, M. Tryby, F. Shang, R. Janke, and T. Haxton. 2020. "EPANET 2.2 User Manual Water Infrastructure Division, Center for Environmental Solutions and Emergency Response."

Seyoum, Alemtsehay G., and Tiku T. Tanyimboh. 2017. "Integration of Hydraulic and Water Quality Modelling in Distribution Networks: EPANET-PMX." *Water Resources Management* 31: 4485–4503.

Summers, Tyler H., Fabrizio L. Cortesi, and John Lygeros. 2016. "On Submodularity and Controllability in Complex Dynamical Networks." *IEEE Transactions on Control of Network Systems* 3 (1): 91–101. https://doi.org/10.1109/TCNS.2015.2453711.

Tryby, Michael E., Dominic L. Boccelli, James G. Uber, and Lewis A. Rossman. 2002. "Facility Location Model for Booster Disinfection of Water Supply Networks." *Journal of Water Resources Planning and Management* 128 (5): 322–33.

Wang, Shen, Ahmad F. Taha, and Ahmed A. Abokifa. 2021. "How Effective Is Model Predictive Control in Real-Time Water Quality Regulation? State-Space Modeling and Scalable Control." *Water Resources Research* 57 (5): e2020WR027771.